Implications of future climate change on crop and irrigation water requirements in a semi-arid river basin using CMIP6 GCMs

Kunal KARAN[1], Dharmaveer SINGH[2*], Pushpendra K SINGH[3*], Birendra BHARATI[1], Tarun P SINGH[2], Ronny BERNDTSSON[4]

[1] Department of Water Engineering and Management, Central University of Jharkhand, Brambe, Ranchi 835205, India;
[2] Symbiosis Institute of Geo-informatics, Symbiosis International (Deemed University), Pune 411016, India;
[3] Water Resources Systems Division, National Institute of Hydrology, Roorkee 247667, India;
[4] Division of Water Resources Engineering & Centre for Advanced Middle Eastern Studies, Lund University, Lund Box 117, 22100, Sweden

Abstract: Agriculture faces risks due to increasing stress from climate change, particularly in semi-arid regions. Lack of understanding of crop water requirement (CWR) and irrigation water requirement (IWR) in a changing climate may result in crop failure and socioeconomic problems that can become detrimental to agriculture-based economies in emerging nations worldwide. Previous research in CWR and IWR has largely focused on large river basins and scenarios from the Coupled Model Intercomparison Project Phase 3 (CMIP3) and Coupled Model Intercomparison Project Phase 5 (CMIP5) to account for the impacts of climate change on crops. Smaller basins, however, are more susceptible to regional climate change, with more significant impacts on crops. This study estimates CWRs and IWRs for five crops (sugarcane, wheat, cotton, sorghum, and soybean) in the Pravara River Basin (area of 6537 km^2) of India using outputs from the most recent Coupled Model Intercomparison Project Phase 6 (CMIP6) General Circulation Models (GCMs) under Shared Socio-economic Pathway (SSP)245 and SSP585 scenarios. An increase in mean annual rainfall is projected under both scenarios in the 2050s and 2080s using ten selected CMIP6 GCMs. CWRs for all crops may decline in almost all of the CMIP6 GCMs in the 2050s and 2080s (with the exceptions of ACCESS-CM-2 and ACCESS-ESM-1.5) under SSP245 and SSP585 scenarios. The availability of increasing soil moisture in the root zone due to increasing rainfall and a decrease in the projected maximum temperature may be responsible for this decline in CWR. Similarly, except for soybean and cotton, the projected IWRs for all other three crops under SSP245 and SSP585 scenarios show a decrease or a small increase in the 2050s and 2080s in most CMIP6 GCMs. These findings are important for agricultural researchers and water resource managers to implement long-term crop planning techniques and to reduce the negative impacts of climate change and associated rainfall variability to avert crop failure and agricultural losses.

Keywords: climate change; crop water requirement; irrigation water requirement; CMIP6 GCMs; emission scenario; Pravara River Basin

Citation: Kunal KARAN, Dharmaveer SINGH, Puspendra K SINGH, Birendra BHARATI, Tarun P SINGH, Ronny BERNDTSSON. 2022. Implications of future climate change on crop and irrigation water requirements in a semi-arid river basin using CMIP6 GCMs. Journal of Arid Land, 14(11): 1234–1257. https://doi.org/10.1007/s40333-022-0081-1

*Corresponding authors: Dharmaveer SINGH (E-mail: veermnnit@gmail.com); Puspendra K SINGH (E-mail: pushpendras123@gmail.com)

Received 2022-07-27; revised 2022-09-10; accepted 2022-09-21

1 Introduction

India's agricultural sector contributes 17.90% to the gross value added and provides employment to 56.40% of the total workforce of the country (Economic Survey, 2021). The Indian agriculture is heavily climate dependent with notable regional and climatic variability, and rain-fed area accounts for approximately 54.00% of the gross cropped area, despite notable efforts to increase the area under irrigation (Gulati et al., 2018). The agricultural sector is facing multi-dimensional pressure from many stressors, such as climate change and socio-economic factors (e.g., population growth, unbounded urbanization, and industrialization) (Dai et al., 2013; Yu et al., 2019). Additionally, potential implications of climate change vary from a regional to local population scale (Farooq et al., 2022). Changes in climate primarily in the forms of rainfall, temperature, and radiation will impact the availability of water resources and water requirements for both irrigated and rain-fed crops (Jain and Singh, 2020). Masia et al. (2021) found that evaporative demand will increase in tandem with rising global temperature, thus increasing crop evapotranspiration. Crop water requirement (CWR) varies depending on the cropping system, and climate change may have a substantial impact on CWR (Sun et al., 2013; Ye et al., 2015). Elgali et al. (2007) found that CWR and irrigation water requirement (IWR) are very sensitive to changes in climatic variables and will vary due to climate change. Thus, climate change is increasingly threatening major crop production systems (Farooq et al., 2022). Ahmad et al. (2021) revealed that the risk of crop failure will be higher due to projected climate change under Coupled Model Intercomparison Project Phase 5 (CMIP5) General Circulation Models (GCMs). However, the actual impacts of climate change on CWR are complex and difficult to predict (Jain and Singh, 2020).

According to the Fifth Assessment Report (AR5) of IPCC (2014), the surface temperature will increase during the 21st century under all emission scenarios and this will adversely impact the agriculture, land and water resources, environment, ecosystems, biodiversity, and even the society (Singh et al., 2015a; Jain and Singh, 2020). Therefore, it is vital to explore the links between agricultural water management and climate change looking into the regional and local variability of food and water security. Döll (2002) applied global irrigation model to assess the impacts of climate change on net IWR and found that there may be an increase in the global net IWR of 5.00%–8.00% by the end of the 2070s and it might be the largest in the South Asia region. Wada et al. (2013) used CMIP5 GCMs and applied seven global hydrological models to evaluate the impacts of climate change on CWR and pointed out that there would be an increase in CWR and a decrease in water availability by the 2080s with pronounced regional patterns. Rehana and Mujumdar (2013) found that there will probably be an increase in CWR due to climate change. Elliot et al. (2014) revealed that there might be an inversion of 2.0×10^4–6.0×10^4 km^2 cropland from irrigated system to rain-fed system due to the limitations of freshwater availability mostly in the irrigated regions of western United States, China, and West, South, and Central Asia.

According to Jain and Singh (2020), the correlation between global CWR and global warming is high and the benefits of increasing rainfall for irrigation is small. Haz-Amor et al. (2020) used CMIP5 GCMs with CROPWAT model and found an increase in IWR based on the scenario projections. Shrestha et al. (2013) also used coupled CROPWAT model with HadCM3 GCM (A2 and B2 scenarios) for future projections and found that IWR varied with physiographic regions and growth stages of crops. The IWRs in the middle and high hills of Nepal were found to have a decreasing trend, while IWR in the Terai region showed an increasing trend. De Silva et al. (2007) predicted the impacts of climate change by coupling CROPWAT model with HadCM3 GCM under A2 and B2 scenarios and found that IWR increased by 23.00% and 13.00% for paddy crop, respectively. Das et al. (2020) assessed the impacts of climate change on crop yield in the eastern Himalayas. More recently, Abdoulaye et al. (2021) and Poonia et al. (2021) assessed the impacts of climate change on CWR and IWR using CROPWAT model coupled with CMIP5 and Coordinated Regional Downscaling Experiment (CORDEX) GCMs, respectively, for river basins in Niger and eastern Himalayan region. Some other important work in this domain includes the

study of Li et al. (2020), who developed a structure for "water suitable" agriculture by analyzing factors affecting IWR. Overall, it can be stated that the climate change-induced increase in water demand will bring further challenges to farmers to irrigate and grow crops with limited water availability. However, the studies done by Flörke et al. (2018) and Gondim et al. (2018) opined that the improvements in agricultural water use efficiency through improved technological and scientific interventions will help to compensate the adverse impacts of climate change and may supply enough water to meet water demands of other sectors. For improving water use efficiency, it is critical to understand how much water crops require at different times of the year, as well as to develop rational irrigation schedule for irrigated areas. Tubiello and Fischer (2007) found that an alleviated climate may reduce the impacts of climate change on agricultural water requirements by about 40.00%, or 125×10^8–160×10^8 m^3, compared with an unmitigated climate. Schwaller et al. (2021) underscore the importance of effective agricultural water management through a comprehensive understanding of CWR and IWR, but this information is frequently not readily available. Therefore, it is of paramount importance to understand the variability of the climate-induced CWRs and IWRs of different crops for effectively managing the agricultural water resources and mitigate the adverse impacts of climate change on agriculture.

However, previous studies, as discussed above, have used climate projections mainly from Coupled Model Intercomparison Project Phase 3 (CMIP3) GCMs and CMIP5 GCMs to assess the future CWR and IWR, which inherited limitations, particularly in simulating the extreme events of rainfall (Kim et al., 2020). This bias in the estimation of rainfall results in higher uncertainties in projected CWR and IWR. More recently, a new generation of Coupled Model Intercomparison Project Phase 6 (CMIP6) framework has been introduced in recent years (Eyring et al., 2016; Gupta et al., 2020; Mishra et al., 2020) to overcome the drawbacks of CMIP3 and CMIP5 models and fulfil the need of a growing climate community. Therefore, in this study, downscaled and bias-corrected GCM outputs of different climatic parameters generated within new Shared Socio-economic Pathways (SSPs) developed as a part of CMIP6 GCM framework were applied for the estimation of CWR and IWR using CROPWAT model for five crops (i.e., sugarcane, cotton, soybean, wheat, and sorghum) of varying growth periods in a semi-arid river basin located in the state of Maharashtra in India for future periods (2050s and 2080s). This study will aid in the understanding of the long-term impacts of climate change on agriculture and the development of adaptation plans for local agricultural water management by local water managers, researchers, and policymakers.

2 Materials and methods

2.1 Study area

The selected study area is the Pravara River Basin (PRB; Fig. 1), located in the Ahmednagar District of Maharashtra State, India. Ahmednagar is one of the worst drought-hit districts in India. It is home to 4.5×10^6 people, of which about 80.00% are rural. Agriculture and animal husbandry are the prime economic activities and contribute significantly to the total income of the region. Pravara River is one of the smallest tributaries of the Godavari River (the second largest river system in Peninsular India) that originates near Akola on the eastern slopes of the Sahyadris (19°31′45″N, 73°45′05″E; 750 m) in the western Ghats. It is a rain-fed and intermittent river that generally dries out in summer. Mahalungi and Mula are two important left and right bank tributaries of the Pravara River that join at Sangamner and Nevasa, respectively.

The river flows approximately 208 km from its origin Sahayadri to its mouth Pravara Sangam (19°37′00″N, 75°01′00″E; 531 m) and forms a basin with an area of approximately 6537 km^2, which is confined between latitude of 19°02′16″–19°41′40″N and longitude of 73°6'1″–75°01′33″E. The entire basin is made up of Cretaceous–Tertiary extrusive basalt flows known as the Deccan Volcanic Province (Wellman and McElhinny, 1970; Alexander, 1981; Widdowson and Mitchel, 1999; Hooper et al., 2010). The major soil category includes shallow alluvium soil, medium black soil, deep black soil, and reddish soil, which account for nearly 38.00%, 48.00%,

13.00%, and 0.80% of the total cultivated area, respectively (http://www.kvk.pravara.com/). Topographically, a moderate relief variation is found in the basin, where altitude ranges from 404 to 1424 m. The western section of the basin has a hilly landscape, whereas the eastern section is a relatively flat plateau. Because of its geographical location, the PRB has a semi-arid climate. The basin's average annual rainfall based on the gridded rainfall data (0.25°×0.25°) of the India Meteorological Department for 30 years (1991–2020) is 593.3 mm. The seasonal monsoonal rains, occurring between June and September, contribute to the majority (about 80.00%) of the total annual rainfall. The annual mean of the maximum temperature (T_{max}) and the minimum temperature (T_{min}) is 34.70°C and 18.90°C, respectively. During summer months (April–June), the maximum daily temperature soars to as high as 49.00°C in the basin. The basin has been brought under intensive agriculture because of the construction of the Bhandardara Dam (height of 507 m, width of 82 m, and capacity of 3.11×10^8 m^3) upstream of the river in 1926. It is one of the major irrigation projects in the Ahmednagar District, accounting for nearly 8.70% (570 km^2) of the total basin area. Sugarcane, cotton, soybean, wheat, and sorghum are important crops that are grown in the region (Table 1). Sugarcane has become the dominant commercial crop in this area, and the Pravara River serves as the primary irrigation source for agriculture. The region is vulnerable to climate change and has experienced persistent multi-year droughts in the recent past. Therefore, it is of paramount importance to understand the variability of the climate-induced CWRs and IWRs of different crops for effectively managing the agricultural water and mitigating the adverse impacts of climate change on agriculture in the PRB.

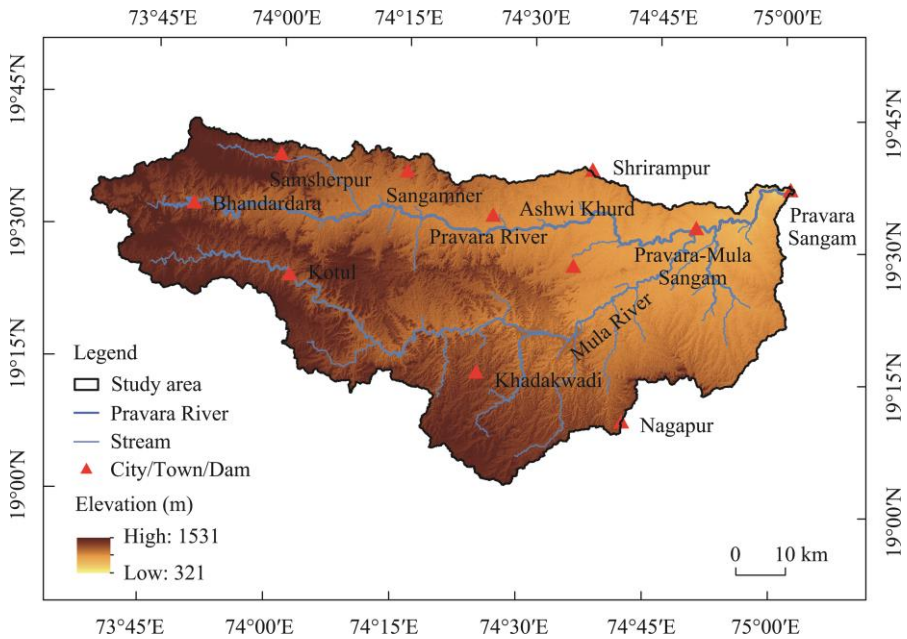

Fig. 1 Overview of the Pravara River Basin (PRB) as well as the important places (cities, towns, and dams) in the basin

Table 1 Planting and harvesting date for the major crops grown in the Pravara River Basin (PRB)

Crop	Scientific name	Planting–harvesting date	Critical depletion factor	Rooting depth (cm)	Length of crop growth stage (d)			
					Initial	Developing	Middle season	Late season
Wheat	Triticum aestivum	15 Oct–11 Feb	0.55	1.50	15	25	50	30
Sorghum	Sorghum bicolor	15 Oct–16 Feb	0.60	1.40	20	35	40	30
Sugarcane	Saccharum officinarum	15 July–14 July	0.65	1.50	30	60	180	95
Cotton	Gossypium	15 July–10 Jan	0.65	1.40	30	50	55	45
Soybean	Glycine max	15 July–1 Dec	0.50	1.00	30	30	50	30

2.2 Agro-meteorological data

Figure 2 shows a schematic on the methodology and data adopted in this study. Data used for the calculations of CWR and IWR including climatic variables, soil parameters, and crop parameters were input in CROPWAT 8.0 model. Meteorological data including temperature (T_{max} and T_{min}), rainfall, wind speed, mean relative humidity, and sunshine hours were obtained on daily time scale for 30 years (1991–2020) from the India Meteorological Department (http://www.imdpune.gov.in/). Rainfall data were available at a grid resolution of 0.250°×0.250°, while other climatic variables were offered at a spatial resolution of 0.500°×0.500°. Soil data (total available moisture content, maximum rain infiltration rate, maximum rooting depth, initial soil moisture depletion, and initial available soil moisture) and crop parameters (planting date, length of crop growth stage, crop coefficient, rooting depth, critical depletion factor, yield response factor, and crop height) were obtained from the Food and Agriculture Organization (FAO) Manual 56 available at http://www.fao.org/land-water/database.

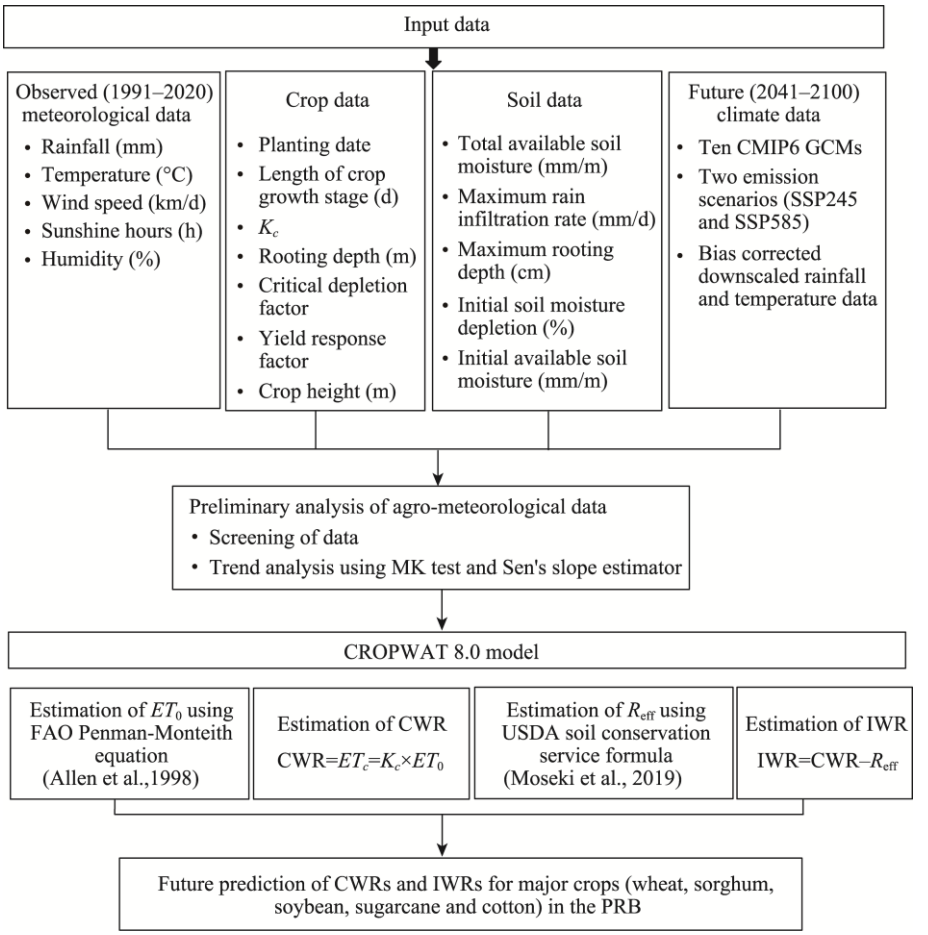

Fig. 2 Flowchart showing the adopted methodology for estimating and investigating the implications of future climate change on CWRs and IWRs for major crops in the PRB. CWR, crop water requirement; IWR, irrigation water requirements; K_c, crop coefficient; CMIP6, Coupled Model Intercomparison Project Phase 6; GCMs, General Circulation Models; SSP, Shared Socio-economic Pathway; MK, Mann-Kendall; ET_0, reference crop evapotranspiration; FAO, Food and Agriculture Organization; ET_c, crop evapotranspiration; R_{eff}, effective rainfall.

2.3 Scenario data of CMIP6 GCMs

In this study, we used the bias corrected downscaled CMIP6 GCM datasets developed by Mishra et al. (2020) for South Asia to investigate the impacts of future climate change on CWR and IWR.

They developed these bias corrected datasets based on Empirical Quantile Mapping approach for the historical (1951–2014) and future (2015–2100) periods under four scenarios: Shared Socio-economic Pathway (SSP)126, SSP245, SSP370, and SSP585. In this study, downscaled high spatial resolution (approximately 0.250°×0.250°) data of ten CMIP6 GCMs (Table 2) were used to reveal the middle (2041–2070) and far (2071–2100) future trends in climatic variables and their implications on CWR and IWR under two scenarios (SSP245 and SSP585) in the PRB. SSPs were used to explain the possible future greenhouse gas emissions under different global socio-economic changes that will take place by 2100 (Riahi et al., 2017). They present socio-economic and technological trajectories with a baseline in which no climate policies are enacted after 2010, resulting in 3.00°C–5.00°C of warming above pre-industrial levels by 2100. In addition, the four SSPs can be linked to climate policies to generate different outcomes at the end of the century (analogous to representative concentration pathways (RCPs)), with radiative forcing of 2.6, 3.4, 4.5, 6.0, 7.0, and 8.5 W/m^2 in 2100.

Table 2 Detailed description of Coupled Model Intercomparison Project Phase 6 (GMIP6) General Circulation Models (GCMs) used in this study

CMIP6 GCM	Description	Spatial resolution	Institution
ACCESS-ESM-1.5	Australian Community Climate and Earth System Simulator-Earth System Model Version 1.0	1.250°×1.875°	Commonwealth Scientific and Industrial Organisation (CSIRO), Australia and Bureau of Meteorology (BOM), Australia
ACCESS-CM-2	Australian Community Climate and Earth System Simulator-Coupled Model Version 2.0	1.250°×1.875°	Commonwealth Scientific and Industrial Organisation (CSIRO), Australia and Bureau of Meteorology (BOM), Australia
BCC-CSM2-MR	Beijing Climate Centre Climate System Model Version 2.0	1.100°×1.100°	Beijing Climate Centre, China Meteorological Administration, China
EC-Earth3	Earth Consortium-Earth 3 Model	0.350°×0.350°	Twenty-seven research institutes from 10 European countries
EC-Earth3-Veg	Earth Consortium-Earth 3 Veg Model	0.350°×0.350°	Twenty-seven research institutes from 10 European countries
INM-CM4-8	Institute for Numerical Mathematics Climate Model Version 4.8	2.000°×1.500°	Institute for Numerical Mathematics, Russia
INM-CM5-0	Institute for Numerical Mathematics Climate Model Version 5.0	2.000°×1.500°	Institute for Numerical Mathematics, Russia
MPI-ESM1-2-HR	Max Planck Institute for Meteorology Earth System Model Version 1.2 with higher resolution	0.940°×0.940°	Max Planck Institute for Meteorology, Germany
MRI-ESM2.0	Meteorological Research Institute Earth System Model Version 2.0	1.125°×1.125°	Meteorological Research Institute, Japan
NorESM2-MM	Norwegian Earth System Model Version 2.0 with medium resolution	2.500°×1.890°	Norwegian Community Earth System Model, Norway

2.4 Screening of data and trend analysis

The inhomogeneity in time series introduces statistical errors that may lead to false analysis and interpretation of climatic events (Peterson et al., 1998; WMO, 2011). Therefore, initial data quality check (e.g., screening data for outliers, trends, and discontinuities) is recommended on time series (monthly, seasonal, and annual) of climatic variables (WMO, 2011). Outliers and inhomogeneity in the historical data were detected using generalized Extreme Studentized Deviate (ESD) test (Rosner, 1983) and Buishand's Range test (Buishand, 1982) methods, respectively. ESD method was used to test the null hypothesis (H_0) that there are no outliers versus the alternative hypothesis (H_1) that there are 'r' outliers in the dataset. The test statistic 'r' was defined by the following equation:

$$r_i = \frac{\max|x_i - \bar{x}|}{s}, \tag{1}$$

where $\bar{x}$, x_i, and s are the sample mean, the i^{th} observation of the sample, and standard deviation, respectively. The r test value is compared with the tabulated critical value at a given level of significance (5% significance level). The null hypothesis that the suspected value is not an outlier is rejected if the r test value is greater than the tabulated critical value. However, in Buishand's Range test method, the test statistic adjusted partial sum (S_k) was calculated by:

$$S_k = \sum_{i=1}^{k} (x_i - \bar{x}) \quad (1 \le i \le n). \tag{2}$$

It is a measure of cumulative deviation from the mean for the k^{th} observation in time series (x_1, x_2, …, x_i, …, x_n). The series is homogenous without any change point if S_k fluctuates around zero. When a break point is present in the series, S_k reaches a maximum value (negative shift) or minimum value (positive shift) for the year $i=k$. The significance of shift was tested using rescaled adjusted range (R) defined by the following equation:

$$R = \frac{\max(S_k) - \min(S_k)}{\bar{x}}. \tag{3}$$

The ratio of R to square root (n) was compared with the tabulated critical values (Buishand, 1982) at given significance level (Table 3). It should be noted that 'n' represents the total number of observations in the time series. The null hypothesis of no change point is rejected if the ratio is less than the critical value (1.43) at 5% significance level. These time series of observations were, further, homogenised using a multistep process based on non-parametric statistics as described in Peterson and Easterling (1994).

Table 3 Statistical information of annual and seasonal climatic variables averaged over 1991–2020 in the PRB

Climatic variable	Mean	Standard deviation	Coefficient of skewness	Coefficient of kurtosis	Coefficient of variance (%)	Buishand's Range test		
						Cumulative deviation/square root (n)	R/square root (n)	Break year
Annual								
T_{max} (°C)	33.72	0.50	–0.27	0.26	1.50	1.38	1.99*	2016
T_{min} (°C)	18.99	0.26	0.04	–0.07	1.40	0.54	0.87	
Rainfall (mm)	593.38	176.10	1.17	1.58	29.68	0.75	0.75	
Pre-monsoon season (March–May)								
T_{max} (°C)	38.99	0.54	0.01	0.46	1.40	1.06	1.50	
T_{min} (°C)	21.07	0.56	–0.37	0.34	2.68	0.58	1.03	
Rainfall (mm)	18.03	22.34	1.88	3.92	123.87	1.09	1.16	
Monsoon season (June–September)								
T_{max} (°C)	31.93	0.69	–0.22	–0.79	2.18	1.37	1.51*	2016
T_{min} (°C)	23.57	0.70	–1.04	0.51	2.99	1.66	1.70*	2016
Rainfall (mm)	470.25	150.39	1.40	2.57	31.98	1.65	1.65*	2017
Post-monsoon season (October–November)								
T_{max} (°C)	32.68	0.88	–0.52	0.63	2.71	1.03	1.53*	2016
T_{min} (°C)	17.77	0.67	–0.08	0.25	3.78	0.89	1.12	
Rainfall (mm)	98.17	75.02	0.94	0.35	76.43	0.89	0.98	
Winter season (December–February)								
T_{max} (°C)	31.49	0.67	–0.01	–0.28	2.13	1.04	1.87*	2019
T_{min} (°C)	11.51	0.93	1.42	1.70	8.11	1.56	1.60*	2017
Rainfall (mm)	6.91	16.81	3.49	13.02	243.05	1.07	1.23	

Note: T_{max}, maximum temperature; T_{min}, minimum temperature; R, rescaled adjusted range.

After the screening of data, the non-parametric (Mann-Kendall (MK)) test and Sen's slope estimator methods were employed for detecting trends in climatic variables. A detailed description of the methods can be found in Singh et al. (2015b).

2.5 Estimations of reference crop evapotranspiration (ET_0), effective rainfall (R_{eff}), CWR, and IWR

CROPWAT 8.0 model was used to estimate ET_0, R_{eff}, and water requirements (CWR and IWR) for the different investigated crops. CROPWAT 8.0 model calculates ET_0, R_{eff}, CWR, and IWR based on climate, crop, and soil data. It has been widely used as a decision-support tool in international settings to calculate regional irrigation needs (Smith et al., 2002; Poonia et al., 2021). The model uses Penman-Monteith (FAO 56 PM) (Savva et al., 2002; Schwallar et al., 2021) equation to calculate ET_0. This equation uses T_{max}, T_{min}, humidity, wind speed, and sunshine hours as input data, and CROPWAT model uses these data to calculate ET_0 by the following expression (Allen et al., 1998):

$$ET_0 = \frac{0.408\Delta(R_n - G) + \gamma \dfrac{900}{T+273} U_2 (e_s - e_a)}{\Delta + \gamma(1+0.34U_2)}, \tag{4}$$

where, ET_0 is the reference crop evapotranspiration (mm/d); R_n is the mean daily net radiation (MJ/(m^2·d)); G is the soil heat flux density (MJ/(m^2·d)); γ is the psychometric constant (0.067 kPa/°C); T is the mean daily air temperature (°C), and the value of $(T_{max}+T_{min})/2$ was measured between 1.5 and 2.0 m height above the ground; U_2 is the wind speed at 2.0 m height above the ground (m/s); e_s is the saturation vapour pressure (kPa); e_a is the actual vapour pressure (kPa); $(e_s–e_a)$ is the vapour pressure deficit (kPa); and Δ is the slope of vapour pressure curve (kPa/°C).

Similarly, R_{eff} was estimated using the following relationship for the two conditions (when R_{month}<250.00 mm and R_{month} >250.00 mm, where R_{month} is the monthly average rainfall (mm)) as described in Moseki et al. (2019):

$$\begin{cases} R_{eff} = R_{month} \times (125 - 0.2 \times R_{month}), \text{ if } R_{month} < 250.00 \text{ mm} \\ R_{eff} = 125 + 0.1 \times R_{month}, \text{ if } R_{month} > 250.00 \text{ mm} \end{cases}. \tag{5}$$

The CWR was calculated using FAO 56 PM equation coupled with the single crop coefficient method as follows (Allen et al., 1998; Luo et al., 2022):

$$ET_c = K_c \times ET_0, \tag{6}$$

where, ET_c and K_c are the crop evapotranspiration (crop water requirement; mm/d) and crop coefficient, respectively. The K_c was determined from the variation in climatic variables, crop types, and growing stages of crops. Notably, in this work, CWR was computed during the whole growth period for all five crops, i.e., sugarcane, wheat, cotton, soybean, and sorghum. Further, IWR was estimated by subtracting R_{eff} from ET_c (Moseki et al., 2019; Poonia et al., 2021):

$$\text{IWR} = ET_c - R_{eff}. \tag{7}$$

3 Results and discussion

3.1 Trends in climatic variables for historical period (1991–2020)

Temporal variability in temperature (T_{max} and T_{min}) and rainfall directly affects the sowing and growing stages of crops. The best way to explain this variability is to look at anomalies in T_{max}, T_{min}, and rainfall and analyze their patterns during the study period (Singh et al., 2016). In this study, anomalies in temperature and rainfall were calculated by subtracting the annual and seasonal time series from the yearly mean averaged for the years 1991–2020 (historical period). Using MK and Sen's slope estimator methods, we determined the magnitudes and directions of changes in T_{max}, T_{min}, and rainfall. The results of MK test (Z_s) and Sen's slope test (Q) are given in

Table 4. At the annual scale, statistically insignificant decreasing trends in T_{max} and rainfall are observed in the PRB for the study period. However, no definite trend in annual T_{min} is detected. Similar patterns are observed for these variables in the post-monsoon but with varying magnitudes. During monsoon, statistically insignificant increasing trends in T_{max} and T_{min} are detected, while rainfall reveals a decreasing trend. However, during winter, no trend in rainfall but a decreasing trend in temperature are observed.

Table 4 Annual and seasonal trends in temperature and rainfall anomalies in the PRB for historical period (1991–2020)

Period	T_{max}		T_{min}		Rainfall	
	Z_s	Q (°C/a)	Z_s	Q (°C/a)	Z_s	Q (°C/a)
Annual	–0.71	–0.01	–0.14	No trend	–1.32	–4.61
Monsoon	0.96	0.02	0.96	0.02	–1.21	–3.78
Pre-monsoon	–0.82	–0.01	0.18	No trend	–0.04	No trend
Winter	–0.71	–0.01	–1.25	–0.02	0.13	No trend
Post-monsoon	–0.71	–0.02	0.86	0.01	–0.25	–0.62

Note: Z_s, Mann-Kendall (MK) test; Q, Sen's slope test.

These results show dissimilarity with previous studies of Guhathakurta et al. (2013) and Singh et al. (2021) where a statistically insignificant decreasing trend of rainfall in winter and an increasing trend of rainfall in pre-monsoon, monsoon, and post-monsoon and annual rainfall are reported in the Ahmednagar District. However, a recent report "Observed Rainfall Variability and Changes over Maharashtra State" published in 2020 by the India Meteorological Department shows a decreasing trend in mean annual and monsoonal rainfall in the Ahmednagar District (Guhathakurta et al., 2020). The difference in these results might be attributed to the length of the data period used for the trend analysis. Specifically, Guhathakurta et al. (2013) and Singh et al. (2021) used long-term gridded data obtained from the India Meteorological Department for 1901–2006 and 1901–2018, respectively, while the data period in the report was 1989–2018. Furthermore, the decreasing trend observed in rainfall can be attributed to the decreased number of rainy days recorded in the Ahmednagar District in the recent decades (1990–2020s).

3.2 Changes in climatic variables under SSP245 and SSP585 scenarios in the 2050s and 2080s

Figures 3 and 4 show projected changes in mean annual T_{max}, T_{min}, and rainfall under SSP245 and SSP585 scenarios for future periods 2041–2070 (2050s) and 2071–2100 (2080s) with respect to the baseline period 1991–2020. All models under both scenarios predict rises in mean annual T_{min} and rainfall in the 2050s and 2080s. The increasing ranges are 0.59°C–3.47°C in the 2050s and 1.21°C–6.47°C in the 2080s for T_{min}, and 11.70%–73.05% in the 2050s and 2.80%–163.80% in the 2080s for rainfall. Within scenarios, relatively high increases in mean annual T_{min} and rainfall are observed under SSP585 scenario compared to SSP245 scenario. However, in general, eight out of ten models predict a decrease in mean annual T_{max} under all scenarios in all future periods except for a higher emission scenario (i.e., SSP585) in the 2080s.

Projected changes in seasonal rainfall under both SSP245 and SSP585 scenarios are investigated. In general, nine out of ten CMIP6 GCMs predict a significant increase in monsoonal rainfall under both scenarios in the 2050s and 2080s. Specifically, the increasing ranges are 21.00%–73.00% in the 2050s and 4.00%–99.00% in the 2080s under SSP245 scenario, and 17.00%–94.00% in the 2050s and 17.00%–176.00% in the 2080s under SSP585 scenario. However, a decrease in post-monsoonal rainfall ranging from –0.02% to –73.00% is projected under SSP245 scenario in the 2050s. Similarly, the analysis of future scenarios in general reveals a decrease in T_{max} for all seasons under a lower emission scenario of SSP245 in the 2050s;

however, an increase in T_{max} is predicted under a higher emission scenario of SSP585 for all seasons in the 2080s. Opposite to this, the increase in T_{min} is predicted for all seasons under both scenarios for most of the models in the 2050s and 2080s. The predicted increase is relatively high for T_{min} as compared to T_{max} under both scenarios for all seasons. The results discussed here are in accordance to previous work of Todmal et al. (2021) who reported increase in mean annual and monsoonal rainfall and minimum temperature over the state of Maharashtra in India for future period (2015–2100) using REgional MOdel (REMO).

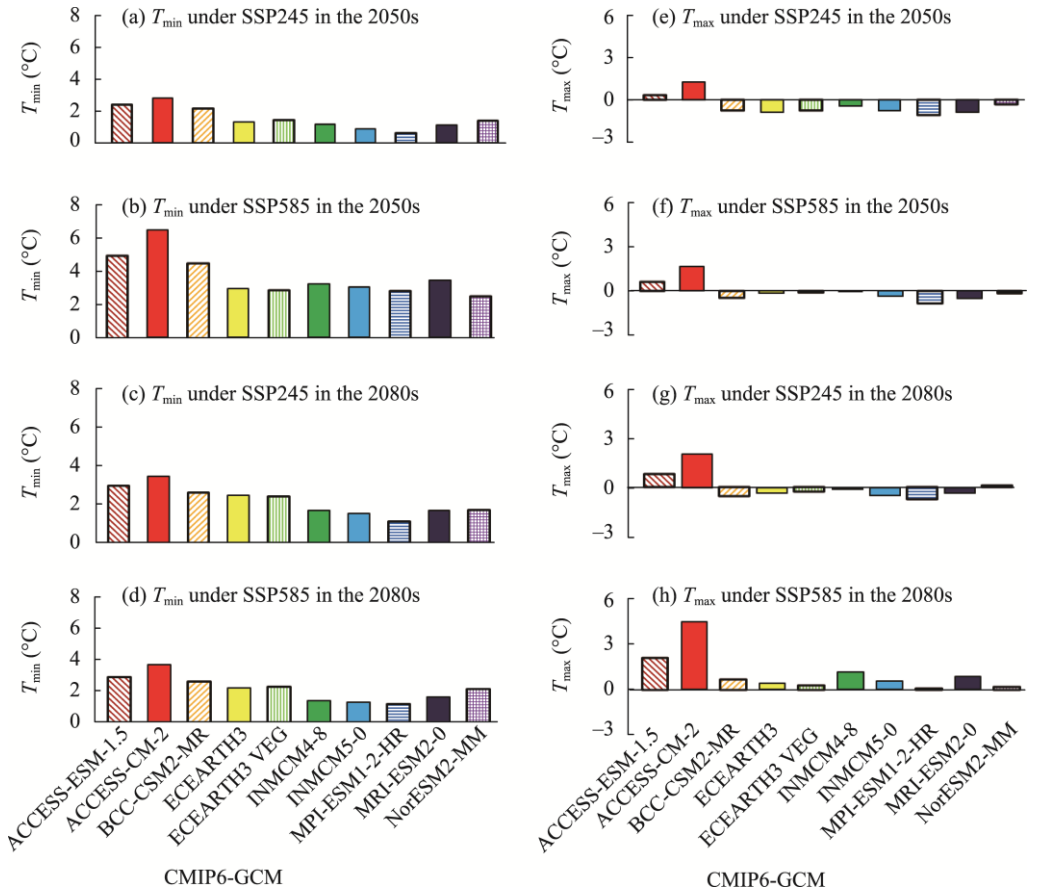

Fig. 3 Projected changes in annual T_{min} (a–d) and T_{max} (e–h) in the PRB using different CMIP6 GCMs under SSP245 and SSP585 scenarios in the 2050s and 2080s. T_{min}, minimum temperature; T_{max}, maximum temperature.

3.3 Estimations of CWR and IWR for historical period (1991–2020)

3.3.1 ET_0 and R_{eff}

Table 5 presents ET_0 and R_{eff} estimated for different months using data of 1991–2020. ET_0 exhibits variations in different months. Due to high temperature in summer, it has the maximum value in April (7.92 mm/d); however, the minimum value occurs in August (4.12 mm/d) as temperature is likewise low in this month. From 1991 to 2020, the long-term yearly average of ET_0 is 5.27 mm/d. The volatility in ET_0 is attributed to changes in other climatic variables. Low humidity, high wind speed, and high temperature cause ET_0 to be at its highest level during the summer season (i.e., dry season). R_{eff} experiences similar variations throughout the year owing to variations in rainfall, with September having the highest value (113.34 mm/month) and January having the lowest value (1.02 mm/month). The long-term (1991–2020) yearly average of R_{eff} is 492.21 mm/month.

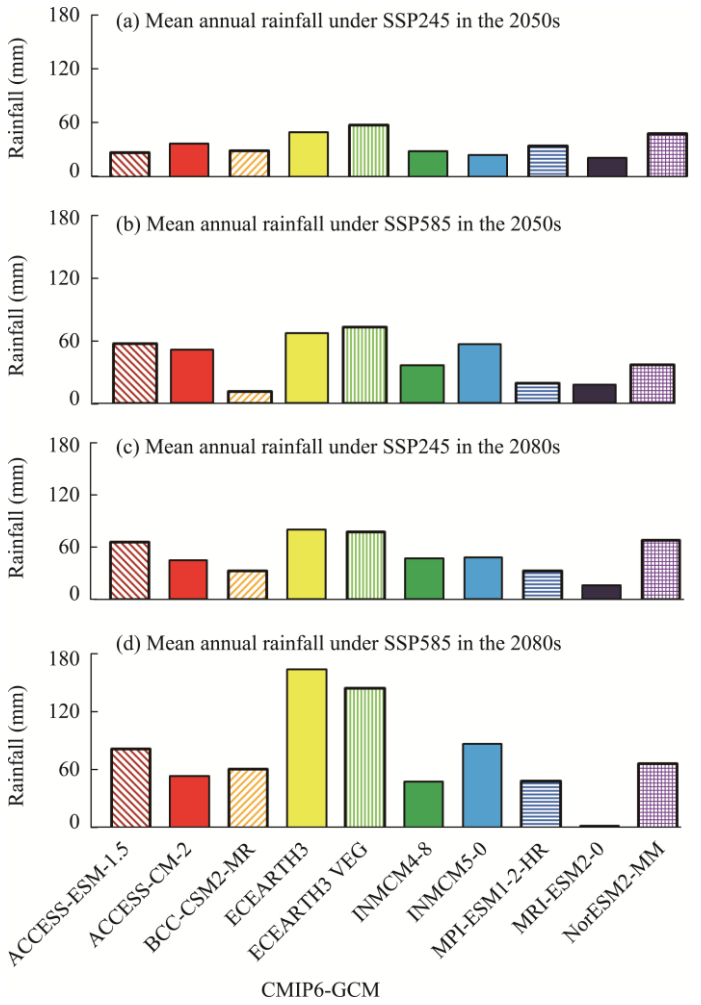

Fig. 4 Projected changes in mean annual rainfall in the PRB using different CMIP6 GCMs under SSP245 and SSP585 scenarios in the 2050s (a and b) and 2080s (c and d).

Table 5 Estimations of monthly reference crop evapotranspiration (ET_0) and effective rainfall (R_{eff}) in the PRB from meteorological data averaged over 1991–2020

Month	Temperature (°C)		Humidity (%)	Wind speed (km/d)	Sunshine hours (h)	R_n (MJ /(m^2·d))	ET_0 (mm/d)	Rainfall (mm/month)	R_{eff} (mm/month)
	T_{min}	T_{max}							
Jan	10.41	30.81	36	182	5.21	13.41	4.44	1.01	1.02
Feb	13.12	33.52	27	203	5.52	15.22	5.54	1.41	1.42
Mar	17.41	37.01	26	233	5.42	16.73	6.80	6.42	6.34
Apr	21.7	39.62	24	291	5.34	17.64	7.92	2.81	2.82
May	24.14	40.42	53	311	5.01	17.44	7.29	8.91	8.82
Jun	24.63	35.12	72	319	5.12	17.52	5.52	115.82	94.34
Jul	23.54	31.01	82	292	5.01	17.35	4.31	98.01	82.62
Aug	23.42	30.21	84	236	5.32	17.52	4.02	107.72	89.13
Sep	22.82	31.62	70	187	5.34	16.81	4.40	148.71	113.34
Oct	20.23	33.42	58	174	5.54	15.62	4.61	77.01	67.56
Nov	15.32	31.92	50	174	5.42	13.91	4.33	21.22	20.51
Dec	11.21	30.41	44	176	5.23	12.82	4.11	4.51	4.53
Average	18.99	33.73	53	232	5.31	16.01	5.27	593.42	492.21

Note: R_n, mean daily net radiation.

3.3.2 Estimations of CWRs and IWRs for different crops

CWR of any crop is the total amount (depth) of water lost owing to evapotranspiration and is determined from ET_c. Every crop has various water requirements depending on the location, climatic conditions, soil type, cultivation technique, and R_{eff} (Ewaid et al., 2019). Tables 6–10 show that R_{eff}, CWR, and IWR fluctuate across the developmental stages of all crops. Moreover, K_c values are not constant at any development stage that indicates seasonal crop water needs (Allen et al., 1998; Azevedo et al., 2007; Irmark et al., 2013). ET_c increases during the growth stage and lowers significantly during the later phases based on K_c values. Tables 6–10 indicate that ET_c values are lower in the early and late stages when crops are in the productive stage and higher in the middle stage. IWRs for all five crops in 10 d are descended in the order of 1707.00 mm/10 d (sugarcane)>500.80 mm/10 d (wheat)>401.60 mm/10 d (cotton)>381.50 mm/10 d (sorghum)>212.80 mm/10 d (soybean), as shown in Tables 6–10.

Table 6 Estimations of CWR and IWR for wheat in the PRB for historical period (1991–2020)

Month	Number of cycles per 10 d	Growth stage	K_c	CWR		R_{eff} (mm/10 d)	IWR (mm/10 d)
				(mm/d)	(mm/10 d)		
Oct	2	Initial	0.75	3.44	20.61	13.50	9.40
Oct	3	Developing	0.75	3.39	37.30	17.30	20.10
Nov	1	Developing	0.88	3.89	38.90	11.10	27.80
Nov	2	Developing	1.06	4.57	45.70	5.40	40.30
Nov	3	Middle	1.19	5.04	50.41	4.10	46.30
Dec	1	Middle	1.19	4.97	49.71	2.90	46.80
Dec	2	Middle	1.19	4.89	48.90	0.90	47.90
Dec	3	Middle	1.19	5.02	55.20	0.70	54.50
Jan	1	Middle	1.19	5.15	51.50	0.60	50.90
Jan	2	Late	1.15	5.10	51.00	0.20	50.80
Jan	3	Late	1.03	4.96	54.60	0.30	54.30
Feb	1	Late	0.91	4.72	47.21	0.30	47.00
Feb	2	Late	0.85	4.72	4.70	0.00	4.70
		Average			555.84	57.30	500.80

Note: K_c, crop coefficient; CWR, crop water requirement; IWR, irrigation water requirement.

Table 7 Estimations of CWR and IWR for sorghum in the PRB for historical period (1991–2020)

Month	Number of cycles per 10 d	Growth stage	K_c	CWR		R_{eff} (mm/10 d)	IWR (mm/10 d)
				(mm/d)	(mm/10 d)		
Oct	2	Initial	0.30	1.38	8.30	13.50	0.00
Oct	3	Initial	0.30	1.35	14.80	17.30	0.00
Nov	1	Developing	0.36	1.59	15.90	11.10	4.80
Nov	2	Developing	0.57	2.45	24.50	5.40	19.20
Nov	3	Developing	0.78	3.32	33.20	4.10	29.20
Dec	1	Middle	0.99	4.14	41.40	2.90	38.50
Dec	2	Middle	1.05	4.31	43.10	0.90	42.20
Dec	3	Middle	1.05	4.43	48.70	0.70	48.00
Jan	1	Middle	1.05	4.55	45.50	0.60	44.80
Jan	2	Late	1.04	4.62	46.20	0.20	46.00
Jan	3	Late	0.92	4.41	48.50	0.30	48.30
Feb	1	Late	0.76	3.95	39.50	0.30	39.20
Feb	2	Late	0.65	3.58	21.50	0.20	21.30
		Average			431.20	57.40	381.50

Table 8 Estimations of CWR and IWR for soybean in the PRB for historical period (1991–2020)

Month	Number of cycles per 10 d	Growth stage	K_c	CWR		R_{eff} (mm/10 d)	IWR (mm/10 d)
				(mm/d)	(mm/10 d)		
Jul	2	Initial	0.40	1.67	10.00	16.00	0.00
Jul	3	Initial	0.40	1.65	18.10	27.70	0.00
Aug	1	Initial	0.40	1.64	16.40	28.50	0.00
Aug	2	Developing	0.47	1.88	18.80	28.90	0.00
Aug	3	Developing	0.72	2.97	32.70	31.90	0.80
Sep	1	Developing	0.98	4.16	41.60	37.30	4.30
Sep	2	Middle	1.13	4.97	49.70	41.10	8.60
Sep	3	Middle	1.14	5.06	50.60	34.90	15.70
Oct	1	Middle	1.14	5.14	51.40	27.60	23.80
Oct	2	Middle	1.14	5.22	52.20	22.50	29.70
Oct	3	Middle	1.14	5.12	56.30	17.30	39.00
Nov	1	Late	1.05	4.60	46.00	11.10	35.00
Nov	2	Late	0.84	3.62	36.20	5.40	30.90
Nov	3	Late	0.63	2.69	26.90	4.10	22.80
Dec	1	Late	0.52	2.17	2.20	0.30	2.20
		Average			509.10	334.40	212.80

Table 9 Estimations of CWR and IWR for sugarcane in the PRB for historical period (1991–2020)

Month	Number of cycles per 10 d	Growth stage	K_c	CWR		R_{eff} (mm/10 d)	IWR (mm/10 d)
				(mm/d)	(mm/10 d)		
Jul	2	Initial	0.81	3.39	20.40	16.00	0.20
Jul	3	Initial	0.40	1.65	18.10	27.70	0.00
Aug	1	Initial	0.40	1.64	16.40	28.50	0.00
Aug	2	Developing	0.44	1.77	17.70	28.90	0.00
Aug	3	Developing	0.60	2.46	27.10	31.90	0.00
Sep	1	Developing	0.76	3.22	32.20	37.30	0.00
Sep	2	Developing	0.91	3.97	39.70	41.10	0.00
Sep	3	Developing	1.06	4.71	47.10	34.90	12.20
Oct	1	Developing	1.21	5.47	54.70	27.60	27.10
Oct	2	Middle	1.31	6.00	60.00	22.50	37.50
Oct	3	Middle	1.31	5.88	64.70	17.30	47.50
Nov	1	Middle	1.31	5.77	57.70	11.10	46.60
Nov	2	Middle	1.31	5.65	56.50	5.40	51.10
Nov	3	Middle	1.31	5.55	55.50	4.10	51.50
Dec	1	Middle	1.31	5.46	54.60	2.90	51.70
Dec	2	Middle	1.31	5.37	53.70	0.90	52.70
Dec	3	Middle	1.31	5.51	60.60	0.70	59.90
Jan	1	Middle	1.31	5.66	56.60	0.60	55.90
Jan	2	Middle	1.31	5.80	58.00	0.20	57.80
Jan	3	Middle	1.31	6.28	69.10	0.30	68.80
Feb	1	Middle	1.31	6.76	67.60	0.30	67.30

To be continued

Continued

Month	Number of cycles per 10 d	Growth stage	K_c	CWR		R_{eff} (mm/10 d)	IWR (mm/10 d)
				(mm/d)	(mm/10 d)		
Feb	2	Middle	1.31	7.24	72.40	0.30	72.10
Feb	3	Middle	1.31	7.79	62.30	0.90	61.40
Mar	1	Middle	1.31	8.34	83.40	1.80	81.60
Mar	2	Middle	1.31	8.89	88.90	2.50	86.40
Mar	3	Middle	1.31	9.38	103.20	2.00	101.20
Apr	1	Middle	1.31	10.05	100.50	1.10	99.40
Apr	2	Late	1.28	10.39	103.90	0.50	103.40
Apr	3	Late	1.23	9.62	96.20	1.30	94.90
May	1	Late	1.17	8.88	88.80	0.30	88.50
May	2	Late	1.12	8.28	82.80	0.00	82.80
May	3	Late	1.06	7.20	79.20	8.60	70.60
Jun	1	Late	1.01	6.15	61.50	25.00	36.50
Jun	2	Late	0.95	5.26	52.60	36.00	16.50
Jun	3	Late	0.90	4.60	46.00	33.20	12.70
Jul	1	Late	0.85	3.92	39.20	28.30	10.90
Jul	2	Late	0.81	3.39	13.60	10.70	0.20
		Average			2162.10	492.40	1707.00

Table 10 Estimations of CWR and IWRs for cotton in the PRB for historical period (1991–2020)

Month	Number of cycles per 10 d	Growth stage	K_c	CWR		R_{eff} (mm/10 d)	IWR (mm/10 d)
				(mm/d)	(mm/10 d)		
Jul	2	Initial	0.35	1.46	8.80	16.00	0.00
Jul	3	Initial	0.35	1.44	15.90	27.70	0.00
Aug	1	Initial	0.35	1.43	14.30	28.50	0.00
Aug	2	Developing	0.40	1.59	15.90	28.90	0.00
Aug	3	Developing	0.57	2.37	26.00	31.90	0.00
Sep	1	Developing	0.75	3.21	32.10	37.30	0.00
Sep	2	Developing	0.93	4.06	40.60	41.10	0.00
Sep	3	Developing	1.10	4.89	48.90	34.90	14.00
Oct	1	Middle	1.21	5.46	54.60	27.60	27.00
Oct	2	Middle	1.21	5.56	55.60	22.50	33.00
Oct	3	Middle	1.21	5.45	59.90	17.30	42.60
Nov	1	Middle	1.21	5.34	53.40	11.10	42.30
Nov	2	Middle	1.21	5.23	52.30	5.40	46.90
Nov	3	Late	1.20	5.09	50.90	4.10	46.80
Dec	1	Late	1.09	4.55	45.50	2.90	42.60
Dec	2	Late	0.97	3.96	39.60	0.90	38.70
Dec	3	Late	0.83	3.51	38.70	0.70	37.90
Jan	1	Late	0.70	3.04	30.40	0.60	29.70
		Average			683.30	339.30	401.60

3.4 Estimations of CWR and IWR for crops under future scenarios

3.4.1 ET_0 and R_{eff}

Using CROPWAT 8.0 model, we calculated ET_0 for different months in the 2050s and 2080s under SSP245 and SSP585 scenarios, as shown in Tables 11 and 12. In the 2050s and 2080s, ET_0 is highest in April and lowest in August as compared to the other months for both the scenarios. The volatility in ET_0 is attributed to changes in climatic variables. Low humidity, high wind speed, and high temperature cause ET_0 to be at its highest level during the summer season (i.e., dry season). Here, it can be deduced that ACCESS-CM-2 GCM consistently projects the highest average ET_0 as compared to the rest of the CMIP6 GCMs under both scenarios, i.e., SSP245 and SSP585, in the 2050s and 2080s.

Table 11 Projected estimations of monthly ET_0 using different CMIP6 GCMs in the PRB under SSP245 and SSP585 scenarios in the 2050s

Month	ET_0 (mm/d)										
	ACCESS-ESM-1.5	ACCESS-CM-2	BCC-CSM 2-MR	EC-EARTH3	EC-EARTH 3 VEG	INMCM4-8	INMCM5-0	MPI-ESM1-2-HR	MRI-ESM2-0	NorESM2-MM	Baseline period
SSP245 scenario											
Jan	4.40	4.47	4.49	4.42	4.44	4.43	4.42	4.41	4.40	4.44	4.44
Feb	5.42	5.56	5.47	5.45	5.51	5.55	5.62	5.39	5.39	5.46	5.54
Mar	6.69	6.86	6.67	6.73	6.72	6.95	6.92	6.59	6.69	6.83	6.80
Apr	7.85	7.89	7.78	7.86	7.81	7.87	7.92	7.72	7.75	7.89	7.92
May	7.16	7.14	7.07	7.11	7.09	6.96	6.90	7.06	7.09	7.08	7.29
Jun	5.62	5.87	5.16	5.71	5.76	5.56	5.50	5.57	5.82	5.56	5.52
Jul	4.25	4.63	4.02	4.23	4.27	4.21	4.21	4.12	6.02	4.21	4.31
Aug	3.94	4.11	3.86	3.94	3.96	4.02	3.94	3.89	3.83	3.95	4.02
Sept	4.58	4.56	4.22	4.23	4.25	4.31	4.20	4.27	4.23	4.22	4.40
Oct	5.00	4.95	4.69	4.36	4.38	4.43	4.37	4.43	4.42	4.53	4.61
Nov	4.55	4.62	4.53	4.13	4.14	4.25	4.20	4.21	4.20	4.38	4.33
Dec	4.18	4.19	4.25	4.03	4.03	4.03	4.07	4.03	4.07	4.14	4.11
Average	5.30	5.40	5.18	5.19	5.20	5.22	5.19	5.14	5.33	5.23	5.27
SSP585 scenario											
Jan	4.46	4.50	4.52	4.45	4.47	4.48	4.46	4.42	4.47	4.50	4.46
Feb	5.49	5.61	5.44	5.53	5.57	5.58	5.68	5.43	5.49	5.55	5.49
Mar	6.73	6.89	6.77	6.80	6.83	6.93	7.02	6.77	6.75	6.90	6.73
Apr	7.93	7.97	7.90	7.98	7.92	7.96	7.94	6.56	7.82	7.96	7.93
May	7.14	7.21	7.02	6.74	7.14	7.01	6.97	7.02	7.09	7.16	7.14
Jun	5.75	5.97	5.19	5.69	5.77	5.64	5.61	5.53	5.86	5.67	5.75
Jul	4.31	4.71	4.06	4.26	4.26	4.28	4.20	5.86	4.34	4.28	4.31
Aug	3.96	4.19	3.89	3.99	4.01	4.05	3.97	3.93	3.88	3.99	3.96
Sept	4.59	4.61	4.25	4.28	4.28	4.35	4.23	4.28	4.27	4.29	4.59
Oct	5.01	5.02	4.74	4.42	4.45	4.47	4.41	4.45	4.46	4.60	5.01
Nov	4.59	4.58	4.58	4.21	4.21	4.31	4.28	4.29	4.24	4.47	4.59
Dec	4.20	4.23	4.29	4.07	4.09	4.15	4.11	4.08	4.08	4.24	4.20
Average	5.35	5.46	5.22	5.20	5.25	5.27	5.24	5.22	5.23	5.30	5.35

Note: The baseline period is from 1991 to 2020.

Table 12 Projected estimations of monthly ET_0 using different CMIP6 GCMs in the PRB under SSP245 and SSP585 scenarios in the 2080s

Month	ET_0 (mm/d)										
	ACCESS-ESM-1.5	ACCESS-CM-2	BCC-CSM2-MR	EC-EARTH3	EC-EARTH3 VEG	INMCM 4-8	INMCM 5-0	MPI-ESM1-2-HR	MRI-ESM2-0	NorESM2-MM	Baseline period
SSP245 scenario											
Jan	4.47	4.55	4.47	4.48	4.53	4.45	4.50	4.44	4.44	4.46	4.44
Feb	5.51	5.64	5.47	5.62	5.67	5.57	5.60	5.44	5.46	5.57	5.54
Mar	6.75	6.91	6.77	6.9	6.87	6.94	7.01	6.68	6.74	6.88	6.80
Apr	7.88	8.01	7.91	7.98	7.95	8.00	7.59	7.84	7.81	7.93	7.92
May	7.19	7.27	7.07	7.17	7.18	7.02	6.94	7.15	7.11	7.18	7.29
Jun	5.77	6.01	5.21	5.81	5.77	5.65	5.58	5.58	5.93	5.74	5.52
Jul	4.34	4.74	4.07	4.29	4.32	4.24	4.20	4.16	4.40	4.28	4.31
Aug	3.95	4.26	3.89	4.01	3.99	4.04	3.96	3.92	3.90	3.98	4.02
Sept	4.58	4.62	4.21	4.28	4.29	4.33	4.22	4.27	4.32	4.27	4.40
Oct	5.03	5.02	4.74	4.38	4.38	4.47	4.39	4.46	4.51	4.55	4.61
Nov	4.61	4.66	4.59	4.17	4.16	4.29	4.22	4.28	4.22	4.44	4.33
Dec	4.27	4.27	4.26	4.06	4.08	4.12	4.09	4.08	4.06	4.22	4.11
Average	5.36	5.5	5.22	5.26	5.27	5.26	5.19	5.19	5.24	5.29	5.27
SSP585 scenario											
Jan	4.63	4.82	4.69	4.65	4.72	4.65	4.61	4.59	4.65	4.69	4.63
Feb	5.68	6.02	5.74	5.91	5.94	5.83	5.77	5.62	5.72	5.83	5.68
Mar	7.06	7.25	6.98	7.17	7.21	7.19	7.15	6.85	7.02	7.14	7.06
Apr	8.23	8.33	8.08	8.21	8.20	8.17	8.15	7.97	8.05	8.19	8.23
May	7.37	7.52	7.23	7.36	7.35	7.16	7.14	7.27	7.29	7.35	7.37
Jun	5.91	6.26	5.37	6.01	5.99	5.79	5.76	5.59	5.97	5.91	5.91
Jul	4.42	5.03	4.13	4.44	4.44	4.38	4.39	4.23	4.42	4.45	4.42
Aug	4.04	4.55	3.96	4.09	4.11	4.12	4.03	4.02	3.95	4.08	4.04
Sept	4.64	4.98	4.34	4.39	4.40	4.42	4.29	4.33	4.36	4.38	4.64
Oct	5.13	5.27	4.86	4.50	4.50	4.61	4.51	4.50	4.64	4.68	5.13
Nov	4.86	4.97	4.71	4.30	4.34	4.51	4.39	4.37	4.40	4.64	4.86
Dec	4.46	4.55	4.44	4.21	4.23	4.27	4.17	4.22	4.27	4.39	4.46
Average	5.54	5.80	5.38	5.44	5.45	5.42	5.36	5.30	5.39	5.48	5.54

Note: The baseline period is from 1991 to 2020.

Further, Figure 5 shows the percentage change in ET_0 under SSP245 and SSP585 scenarios in the 2050s and 2080s. For all of the CMIP6 GCMs, the percentage change in ET_0 is negative (i.e., ET_0 is decreasing) under SSP245 scenario in the 2050s and 2080s, except for the three CMIP6 GCMs, i.e., ACCESS-CM-2, MRI-ESM2-0, and ACCESS-ESM-1.5, in which the percentage change in ET_0 is positive, i.e., 2.70% and 4.60%, respectively, in the 2050s and 2080s with respect to average ET_0 in the baseline period (1991–2020). Specifically, in the 2080s, only two CMIP6 GCMs (i.e., ACCESS-CM-2 and ACCESS-ESM-1.5) predict a positive increase in ET_0 under SSP245 scenario. Mondal et al. (2021) reported an increase of 4.00% in ET_0 over the Indus River Basin under the medium emission scenario (SSP245). A similar pattern is observed under SSP585 scenario in the 2050s in this study, where for almost all of the CMIP6-GCMs, the percentage change in ET_0 is negative (i.e., ET_0 is decreasing), except for the two CMIP6 GCMs, i.e., ACCESS-CM-2 and ACCESS-ESM-1.5, in which the percentage change in ET_0 is positive,

i.e., 3.80% and 1.70%, respectively, with respect to average ET_0 in the baseline period (1991–2020). However, under SSP585 scenario in the 2080s, all of CMIP6 GCMs reveal consistently a positive change in ET_0 (i.e., ET_0 is increasing), up to 20.30%, which is much higher than the percentage increase in ET_0 (4.60%) under SSP245 scenario in the 2080s. Overall, ET_0 is predicted to increase for all ten CMIP6 GCMs under SSP585 scenario (high emission scenario) in the 2080s, while both increasing and declining trends are observed with decreasing pronounced pattern for the remaining periods and scenarios.

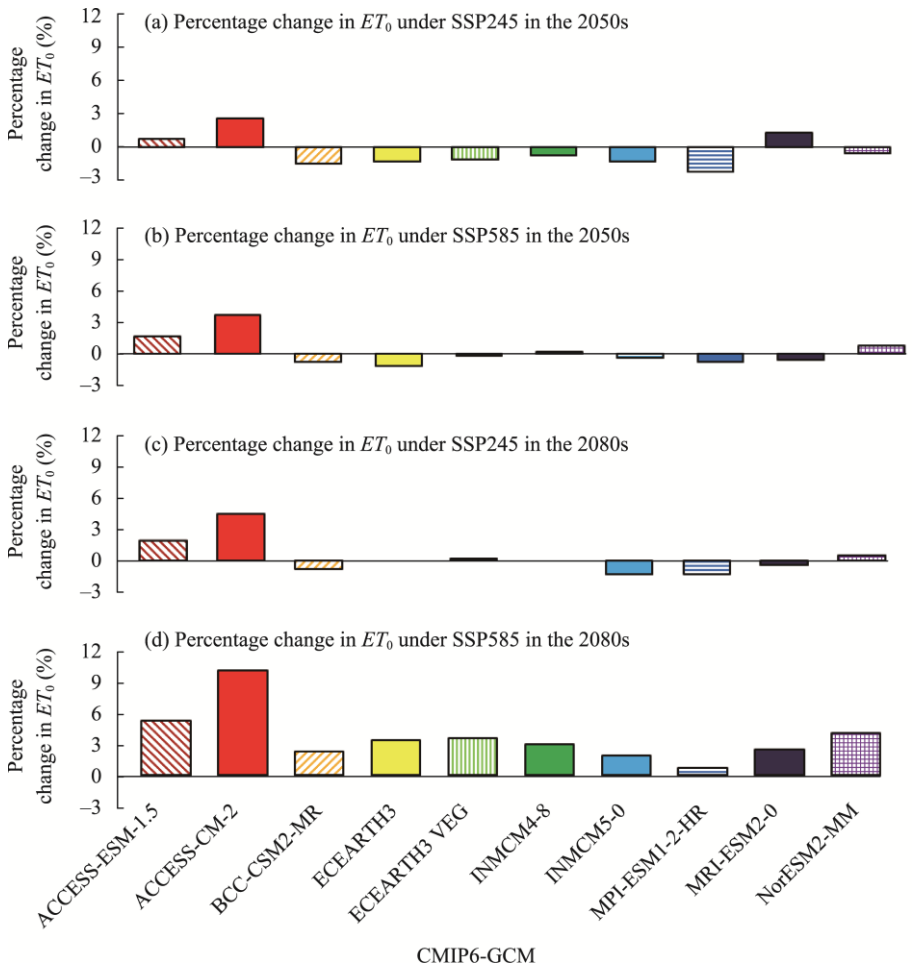

Fig. 5 Projected percentage change in ET_0 using different CMIP6 GCMs in n the PRB under SSP245 (a and b) and SSP585 (c and d) scenarios in the 2050s and 2080s

3.4.2 Estimations of CWRs and IWRs for different crops

Table 13 shows CWR estimates for different crops using ten CMIP6 GCMs under two scenarios, i.e., SSP245 and SSP585, in the 2050s and 2080s. It can be observed from Table 13 that two CMIP6 GCMs, namely ACCESS-CM-2 and ACCESS-ESM-1.5, project increases in CWRs for cotton and soybean crops under both SSP245 and SSP585 scenarios as compared to the rest of the eight CMIP6 GCMs, which estimate decreases in CWRs for all crops in the 2050s and 2080s. However, the overall averages of projected CWRs for cotton, sorghum, sugarcane, soybean, and wheat for all ten models are 667.80, 417.20, 2102.40, 501.20, and 542.80 mm in the 2050s, and 671.70, 420.50, 2112.40, 500.90, and 547.50 mm in the 2080s, respectively. These values are comparatively lower than those during historical period (1991–2020). Figure 6 also shows the projected percentage change (percentage increase or decrease) of CWRs for all crops using the

ten CMIP6 GCMs under SSP245 and SSP585 scenarios in the 2050s and 2080s, with respect to the baseline period 1991–2020. With the exceptions of ACCESS-CM-2 and ACCESS-ESM-1.5, which predict increases of CWRs in soybean, cotton, and wheat under SSP245 scenario in the 2050s and 2080s, decreases in the estimated percentage change of CWRs for all crops are found for nearly all of the CMIP6 GCMs. Similarly, under SSP585 scenario, there are decreases in the projected percentage change of CWRs for almost all of the CMIP6 GCMs in the 2050s, except for ACCESS-CM-2 and ACCESS-ESM-1.5. However, a detailed analysis shows that there exist increases in the projected percentage change of CWRs for all crops under SSP585 scenario in the 2080s as compared to the SSP245 scenario in the 2050s. This could be related to the rise in T_{max} during this period. Additionally, results of ACCESS-CM-2 and ACCESS-ESM-1.5 indicate that there are larger increases in the projected percentage change of CWRs for soybean, cotton, and wheat than for sugarcane and sorghum under both scenarios in the 2050s and 2080s. Overall, the results show that the projected percentage change of CWR is decreasing for almost all of CMIP6 GCMs (except for ACCESS-CM-2 and ACCESS-ESM-1.5) under SSP245 scenario in the 2050s and 2080s. However, under SSP585 scenario, the projected percentage change of CWRs for all crops may increase for five GCMs (ACCESS-ESM-1.5, ACCESS-CM-2, BCC-CSM2-MR, INMCM4-8, and NorESM2-MM) in the 2080s. As an example, by using MRI-ESM2-0, the projected percentage change of CWR for sugarcane is –2.30%, whereas the values are –4.60%, –3.90%, –3.60%, and –2.30%, respectively, for sorghum, wheat, cotton, and soybean.

Table 13 Projected CWRs of five crops using different CMIP6 GCMs in the PRB under SSP245 and SSP585 scenarios in the 2050s and 2080s

CMIP6 GCM	Scenario	Average CWR (mm)									
		2050s					2080s				
		Cotton	Sorghum	Sugarcane	Soybean	Wheat	Cotton	Sorghum	Sugarcane	Soybean	Wheat
ACCESS-ESM-1.5	SSP245	702.80	419.30	2123.20	534.30	551.90	708.30	425.50	2144.90	536.60	559.90
	SSP585	703.30	421.10	2133.40	535.30	554.80	726.50	435.90	2199.20	547.90	576.80
ACCESS-CM-2	SSP245	710.80	426.00	2166.70	539.70	559.80	720.70	430.60	2193.50	548.40	566.10
	SSP585	713.00	426.70	2177.80	542.70	560.80	761.80	453.10	2295.30	581.10	596.90
BCC-CSM2-MR	SSP245	673.60	426.10	2076.50	502.80	555.80	674.20	425.10	2069.00	501.80	556.10
	SSP585	678.90	427.80	2086.60	506.40	559.10	694.40	437.70	2131.70	517.00	573.50
EC-EARTH3	SSP245	644.60	411.40	2079.50	482.60	531.90	647.00	414.60	2099.20	458.30	536.10
	SSP585	649.00	412.80	2073.50	486.80	535.50	659.10	425.80	2144.40	496.10	552.30
EC-EARTH3 VEG	SSP245	646.30	411.70	2080.70	484.80	532.70	648.90	416.20	2099.20	485.90	538.30
	SSP585	650.60	414.90	2093.10	488.50	537.70	654.20	420.80	2133.40	492.60	546.70
INMCM4-8	SSP245	664.70	412.60	2106.50	496.90	536.80	673.00	418.60	2128.00	501.50	544.10
	SSP585	673.80	420.20	2126.50	500.70	546.80	695.20	436.40	2191.10	513.60	567.30
INMCM5-0	SSP245	655.20	417.30	2102.50	485.40	540.20	658.30	419.90	2093.30	487.70	543.40
	SSP585	662.60	420.70	2119.30	490.20	545.30	673.50	427.60	2156.80	498.20	555.30
MPI-ESM1-2-HR	SSP245	654.80	414.10	2070.90	490.50	536.40	658.50	417.70	2084.90	493.00	541.50
	SSP585	667.50	417.20	2052.80	503.40	540.80	666.40	425.30	2109.80	498.50	552.30
MRI-ESM2-0	SSP245	659.00	411.40	2113.40	497.50	533.90	656.30	412.90	2092.40	494.50	536.90
	SSP585	653.70	413.40	2086.20	490.90	537.40	672.30	424.30	2138.80	505.70	553.80
NorESM2-MM	SSP245	666.90	421.60	2103.60	497.40	548.10	671.80	424.00	2120.00	501.30	552.20
	SSP585	676.40	426.00	2123.20	505.00	555.10	693.60	438.30	2181.30	516.80	572.30

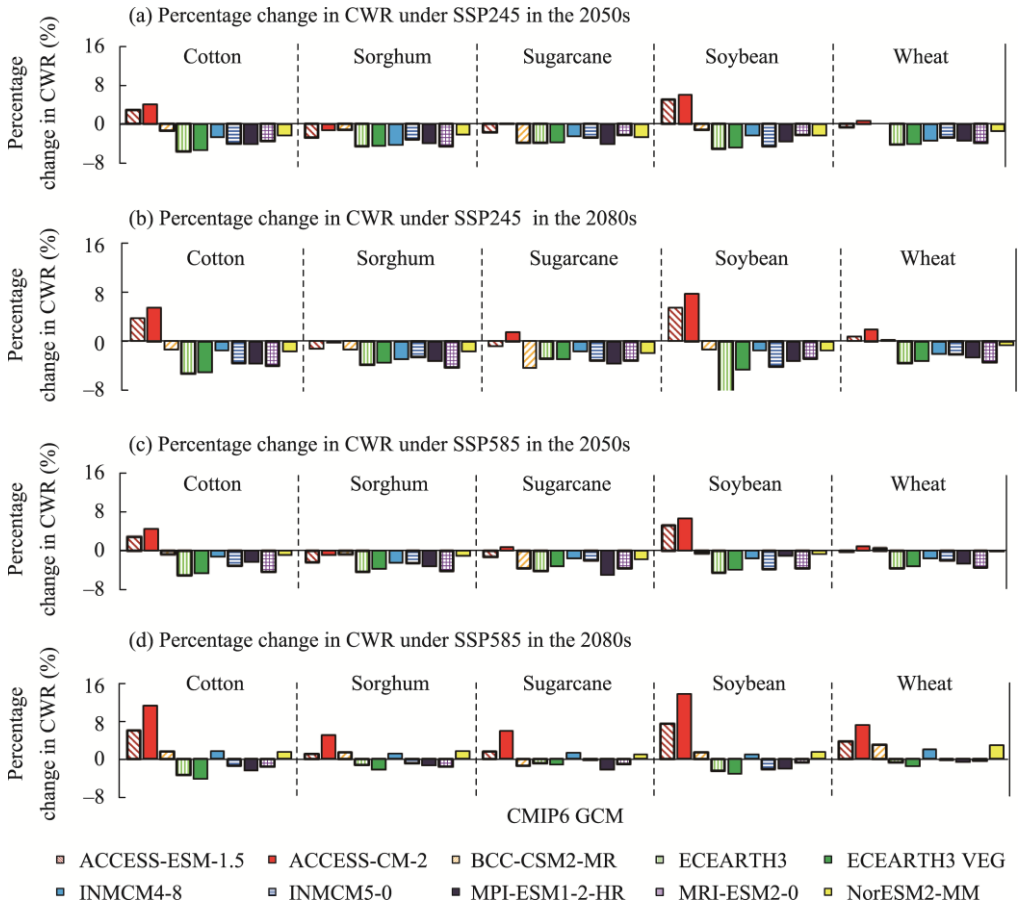

Fig. 6 Projected percentage change in CWRs of five crops using different CMIP6 GCMs in the PRB under SSP245 (a and b) and SSP585 (c and d) scenarios in the 2050s and 2080s

However, the overall averages of the projected percentage decrease of CWRs for all five crops using the ten CMIP6 GCMs reveal that cotton has the largest percentage decrease of CWR (–3.70%), followed by sorghum (–3.60%), sugarcane (–3.30%), soybean (–3.30%), and wheat (–2.9%) under SSP245 scenario in the 2050s and 2080s (Fig. 6), with respect to the baseline period (1991–2020) as given in Tables 6–10. Similarly, under SSP585 scenario, sugarcane shows the largest percentage decrease in projected CWR (–3.10%), followed by cotton (–2.80%), sorghum (–2.80%), soybean (–2.50%), and wheat (–2.00%) (Fig. 6). This indicates that the pattern of the percentage decrease in CWRs for all five crops is similar in the 2050s under both scenarios (i.e., SSP245 and SSP585), except for sugarcane, which shows a larger percentage decrease in CWRs under SSP585 scenario in the 2050s as compared to the other crops. Similarly, in the 2080s, the overall averages of the projected percentage decrease of CWRs for all five crops using the ten CMIP6 GCMs show that soybean exhibits the largest percentage decrease in projected CWR (–3.70%), followed by cotton (–3.30%), sugarcane (–3.00%), sorghum (–2.90%), and wheat (–2.20%) under SSP245 scenario. The availability of increasing soil moisture in the root zone due to increasing rainfall and a decrease in projected T_{max} may be responsible for this decline in CWR.

Figure 6 indicates that the percentage decreases in CWR for wheat crop under both SSP245 and SSP585 scenarios in the 2050s and 2080s are lower as compared to the other crops for most of the CMIP6 GCMs, in which CWR is projected to increase. This shows that crops like wheat and sugarcane will have higher CWRs in future than other crops in the PRB. However, at the same time, if we look into the CWRs projected by ACCESS-ESM-1.5 and ACCESS-CM-2 GCMs, CWRs of cotton and soybean will increase under both SSP245 and SSP585 scenarios in the 2050s

and 2080s. Acharjee et al. (2017) found that future CWRs are projected to fluctuate and depend on the rainfall pattern. Overall, our results imply that projected CWRs are decreasing for most of the CMIP6 GCMs (except for ACCESS-CM-2 and ACCESS-ESM-1.5) under SSP245 scenario in the 2050s and 2080s. However, under SSP585 scenario, projected CWRs for all crops show increases for half of the CMIP6 GCMs in the 2080s in comparison to the 2050s. This analysis indicates that crops such as wheat and sugarcane have lower decreases in CWRs as compared to other crops in the PRB in comparison to the baseline period (1991–2020).

Table 14 shows the estimations of future IWRs for the five selected crops using ten CMIP6 GCMs under two different scenarios, i.e., SSP245 and SSP585, in the 2050s and 2080s. The overall averages of projected IWRs for cotton, sorghum, sugarcane, soybean, and wheat in the 2050s for all CMIP6 GCMs are 415.00, 357.30, 1730.70, 249.60, and 471.10 mm under SSP245 scenario, and 367.40, 317.80, 1562.90, 213.10, and 430.00 mm under SSP585 scenario, respectively. Similarly, projected IWRs in the 2080s are 405.30, 350.60, 1720.80, 230.80, and 474.40 mm under SSP245 scenario, and 354.30, 318.30, 1575.80, 196.9, and 427.5 mm under SSP585 scenario, for cotton, sorghum, sugarcane, soybean, and wheat crops. In general, there is a decrease in the overall projected IWRs for both scenarios in the 2050s and 2080s with respect to baseline period (1991–2020). We evaluated the percentage deviation between the overall average of projected IWRs for all five crops under SSP245 and SSP585 scenarios with respect to the baseline period (1991–2020). The results show that under SSP245 scenario, sorghum has the largest percentage decrease in projected IWR (–6.30%), followed by wheat (–5.90%) as compared to the other crops, whereas soybean has the largest percentage increase in projected IWR (17.30%), followed by cotton (3.30%) in the 2050s. Under SSP585 scenario, again, sorghum crop

Table 14 Projected IWRs of five crops using different CMIP6 GCMs in the PRB under SSS245 and SSP585 scenarios in the 2050s and 2080s

CMIP6 GCM	Scenario	Average IWR (mm)									
		2050s					2080s				
		Cotton	Sorghum	Sugarcane	Soybean	Wheat	Cotton	Sorghum	Sugarcane	Soybean	Wheat
ACCESS-ESM-1.5	SSP245	453.90	395.90	1755.20	319.60	430.20	443.50	311.90	1763.90	296.40	447.00
	SSP585	397.30	259.00	1713.00	293.80	392.00	392.40	275.40	1720.90	270.10	418.30
ACCESS-CM-2	SSP245	416.30	286.20	1724.10	289.80	422.70	404.90	316.30	1724.00	243.00	451.00
	SSP585	374.20	290.00	1683.10	218.30	409.70	350.90	266.00	1718.90	224.70	381.90
BCC-CSM2-MR	SSP245	499.80	408.80	1732.50	317.20	538.70	452.50	402.00	1686.90	264.50	533.30
	SSP585	495.80	411.20	1757.10	310.30	542.60	497.50	417.70	1759.10	302.20	553.80
ECEARTH3	SSP245	352.60	353.20	1680.90	172.90	468.20	348.80	354.60	1682.90	163.10	471.20
	SSP585	346.90	356.30	1655.30	168.60	470.60	286.70	341.20	1659.00	113.10	438.60
ECEARTH3 VEG	SSP245	360.10	350.10	1686.50	176.90	470.80	356.20	356.80	1680.90	173.00	475.70
	SSP 585	365.60	355.20	1695.00	182.20	478.10	305.40	352.70	1665.60	117.50	453.30
INMCM4-8	SSP245	454.70	314.00	1808.30	322.00	438.20	475.30	329.90	1814.30	317.30	455.40
	SSP585	472.70	349.40	1834.50	314.60	477.40	502.90	380.40	1884.30	329.50	511.30
INMCM5-0	SSP245	445.30	370.80	1812.80	277.00	493.80	428.10	373.30	1767.50	253.40	495.00
	SSP585	431.80	376.10	1802.20	248.50	500.80	396.30	354.80	1770.90	219.50	473.10
MPI-ESM1-2-HR	SSP245	389.20	378.10	1702.60	196.20	495.80	399.20	379.70	1666.90	205.10	504.50
	SSP585	396.30	382.40	1642.30	202.20	503.20	364.20	396.60	1646.50	162.60	503.90
MRI-ESM2-0	SSP245	397.30	337.20	1739.20	238.90	458.80	364.20	310.40	1710.80	210.90	416.70
	SSP585	371.90	344.10	1710.70	208.00	461.70	417.80	334.60	1774.40	248.70	463.30
NorESM2-MM	SSP245	380.60	379.10	1664.60	185.30	493.80	380.40	371.10	1709.90	181.30	493.90
	SSP585	389.30	371.50	1698.40	197.70	493.50	383.10	381.40	1733.70	178.10	505.20

crop has the largest decrease in projected IWR (–16.70%) with respect to the baseline period, followed by wheat (–14.40%), cotton (–8.50%), and sugarcane (–8.40%) in the 2050s.

Similarly, Figure 7 shows the projected percentage change in IWRs for all crops under SSP245 and SSP585 scenarios in both periods. In general, the projected percentage change of IWRs for all crops under SSP245 and SSP585 scenarios are decreasing or slightly increasing, except for soybean and cotton, which have the largest increase in IWRs (up to 51.30% and 24.50%, respectively) in the 2050s under SSP245 scenario. Sorghum has the largest percentage decrease in IWR (–25.00%) in the 2050s under SSP245 and SSP585 scenarios (Fig. 7). Similar pattern (with slight increase or decrease) is observed for this crop in the 2080s under both scenarios. The main reason for the decrease in projected IWR may be attributed to the increase in average annual rainfall. The projected percentage change of IWR show high variations under SSP245 and SSP585 scenarios in the 2050s and 2080s mainly due to large variability in projected rainfall. Figure 7 further indicates that in general there are increases in the projected percentage change of IWRs in the 2050s and 2080s under both scenarios for soybean and cotton by using five CMIP6 GCMs (ACCESS-ESM-1.5, ACCESS-CM-2, BCC-CSM2-MR, INMCM4-8, and INMCM5.0). Konzmann et al. (2013) observed that increased rainfall resulted in a modest drop in irrigation needs in several regions worldwide, including southeastern China and India. There is also the argument that the structural crop responses caused by elevated CO_2 concentrations may offset the negative impacts of climate change on agriculture, which would result in lower IWRs in many parts of the world (Konzmann et al., 2013).

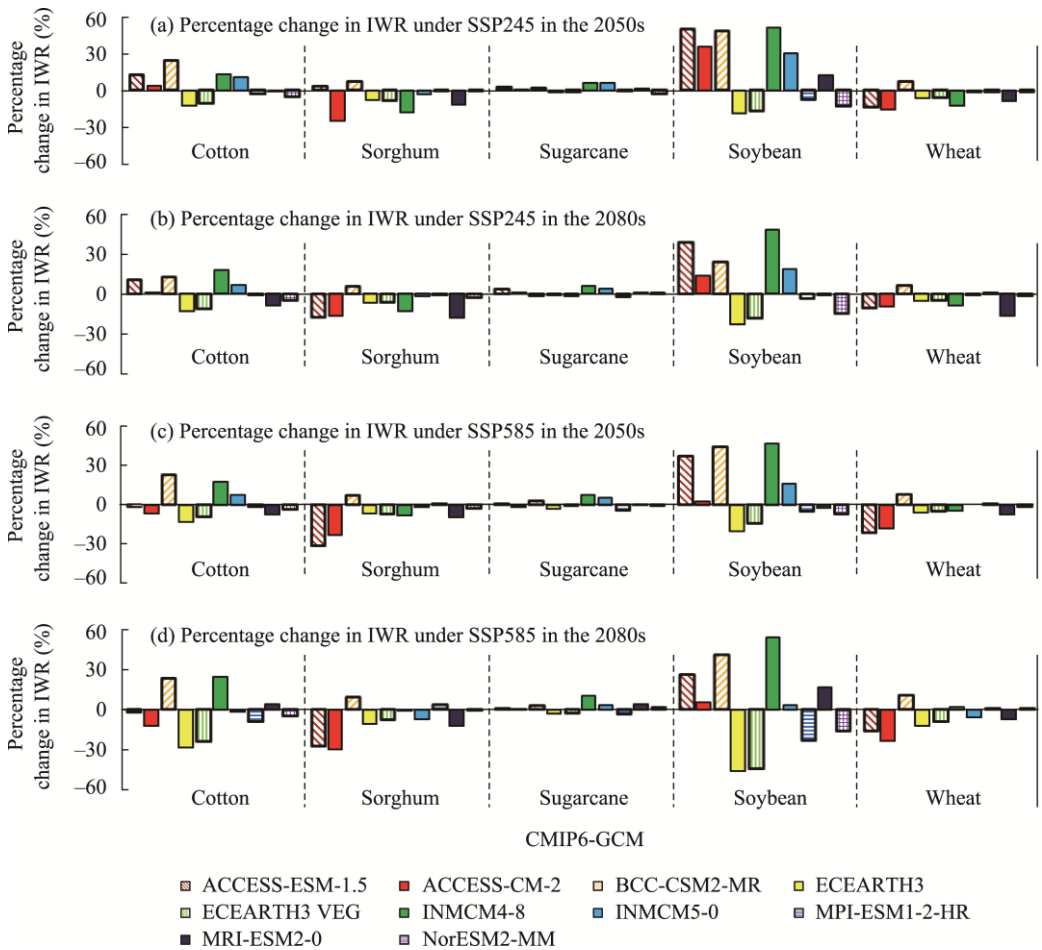

Fig. 7 Projected percentage change in IWRs using different CMIP6 GCMs in the PRB under SSP245 (a and b) and SSP585 (c and d) scenarios in the 2050s and 2080s

4 Conclusions

In this study, multi-scenario projections from CMIP6 GCMs were used to investigate the impacts of climate change on CWR and IWR in a semi-arid river basin of India under two future scenarios (SSP245 and SSP585) in the 2050s and 2080s. We found that projected CWRs decrease for all five crops for almost all of the CMIP6 GCMs (except for ACCESS-CM-2 and ACCESS-ESM-1.5 for soybean and cotton) under SSP245 and SSP585 scenarios in the 2050s and 2080s. This increase in CWRs observed for ACCESS-CM-2 and ACCESS-ESM-1.5 under both scenarios, i.e., SSP245 and SSP585, is more pronounced in the 2080s. The study also found that CWRs in crops such as sugarcane, sorghum, and wheat would decrease for all ten CMIP6 GCMs under both scenarios in the 2050s and 2080s. This could be attributed to the projected decrease in T_{max}. Similarly, projected IWRs for all five crops under SSP245 scenario would decrease or slightly increase in the 2050s and 2080s, except for soybean and cotton. For about four CMIP6 GCMs (EC-Earth3, EC-Earth-veg, MPI-ESM1-2-HR, and NorESM2-MM), a decrease in IWR is found in the 2050s and 2080s under both scenarios. Sorghum crop has the largest decrease in IWR in the 2050s and 2080s under both scenarios, followed by wheat and sugarcane. However, at the same time, soybean exhibits the largest increase in IWR in the 2050s and 2080s under both scenarios, followed by cotton. The main reason for the drop in IWRs may be attributed to the increase in average annual rainfall. The results further show that crops like cotton and soybean are more vulnerable to climate change than other crops in the PRB. This implies that farmers may opt to increase the acreage of sorghum and wheat as compared to soybean and cotton. These results will be of great assistance to agricultural researchers and water resource managers in adopting long-term crop planning techniques to lessen the detrimental impacts of climate change on water resources management in agricultural semi-arid regions like the PRB.

Acknowledgements

This study is supported by the research project Developing Localized Indicators of Climate Change for Impact Risk Assessment in Ahmednagar using CMIP5 Data through University Grant Commission-Basic Science Research (UGC-BSR) Start-Up Grant (No. F. 30-525/2020 (BSR)). We acknowledge University Grant Commission, New Delhi for providing fund. We also extend our gratitude to two anonymous reviewers and editors for their constructive comments and great support during the revision of this paper.

References

Abdoulaye A O, Lu H, Zhu Y et al. 2021. Future irrigation water requirements of the main crops cultivated in the Niger River Basin. Atmosphere, 12(4): 439, doi: 10.3390/atmos12040439.

Acharjee T K, Ludwig F, van Halsema G, et al. 2017. Future changes in water requirements of Boro rice in the face of climate change in North-West Bangladesh. Agricultural Water Management, 194: 172–183.

Ahmad M J, Cho G H, Kim S H, et al. 2021. Influence mechanism of climate change over crop growth and water demands for wheat-rice system of Punjab, Pakistan. Journal of Water and Climate Change, 12(4): 1184–1202.

Alexander P O. 1981. Strontium-isotopic composition of Dhandhuka basalts, western India. Chemical Geology, 32(1–4): 129–138.

Allen R G, Pereira L S, Raes D, et al. 1998. Crop evapotranspiration - Guidelines for computing crop water requirements - FAO Irrigation and drainage paper 56. Food and Agriculture Organization of the United Nations (FAO), Rome, 300(9): D05109. [2022-07-15]. https://www.fao.org/3/x0490e/x0490e00.htm.

Buishand T A. 1982. Some methods for testing the homogeneity of rainfall records. Journal of Hydrology, 58(1–2): 11–27.

Dai S, Li L, Xu H, et al. 2013. A system dynamics approach for water resources policy analysis in arid land: a model for Manas River Basin. Journal of Arid Land, 5(1): 118–131.

Das J, Poonia V, Jha S, et al. 2020. Understanding the climate change impact on crop yield over Eastern Himalayan Region: ascertaining GCM and scenario uncertainty. Theoretical and Applied Climatology, 142(1): 467–482.

de Azevedo P V, de Souza C B, da Silva, B B et al. 2007. Water requirements of pineapple crop grown in a tropical environment, Brazil. Agricultural Water Management, 88(1–3): 201–208.

De Silva C S, Weatherhead E K, Knox J W, et al. 2007. Predicting the impacts of climate change—A case study of paddy

irrigation water requirements in Sri Lanka. Agricultural Water Management, 93(1–2): 19–29.

Döll P. 2002. Impact of climate change and variability on irrigation requirements: a global perspective. Climatic Change, 54(3): 269–293.

Economic Survey. 2021. Economic Survey 2020–2021. [2022-08-15]. https://www.indiabudget.gov.in/economicsurvey/ebook_es2021/index.html.

Elgaali E, Garcia L A, Ojima D S, et al. 2007. High resolution modeling of the regional impacts of climate change on irrigation water demand. Climatic Change, 84: 441–461.

Elliott J, Deryng D, Müller C, et al. 2014. Constraints and potentials of future irrigation water availability on agricultural production under climate change. Proceedings of the National Academy of Sciences, 111(9): 3239–3244.

Ewaid S H, Abed S A, Al-Ansari N. 2019. Crop water requirements and irrigation schedules for some major crops in Southern Iraq. Water, 11(4): 756, doi: 10.3390/w11040756.

Eyring V, Bony S, Meehl G A, et al. 2016. Overview of the Coupled Model Intercomparison Project Phase 6 (CMIP6) experimental design and organization. Geoscientific Model Development, 9(5): 1937–1958.

Farooq M S, Uzaiir M, et al. 2022. Uncovering the research gaps to alleviate the negative impacts of climate change on food security: A review. Frontiers in Plant Science, 13: 927535, doi: 10.3389/fpls.2022.927535.

Flörke M, Schneider C, McDonald R I. 2018. Water competition between cities and agriculture driven by climate change and urban growth. Nature Sustainability, 1(1): 51–58.

Gondim R, Silveira C, de Souza Filho F, et al. 2018. Climate change impacts on water demand and availability using CMIP5 models in the Jaguaribe basin, semi-arid Brazil. Environmental Earth Sciences, 77(15): 1–14.

Guhathakurta P, Saji E. 2013. Detecting changes in rainfall pattern and seasonality index vis-à-vis increasing water scarcity in Maharashtra. Journal of Earth System Science, 122(3): 639–649.

Guhathakurta P, Khedika S, Menon P, et al. 2020. Observed rainfall variability and changes over Maharashtra State. Met Monograph No. ESSO/IMD/HS/Rainfall Variability/16 (2020)/40, India Meteorological Department, Pune. [2021-10-15]. https://imdpune.gov.in/hydrology/rainfall%20variability%20page/maharashtra_final.pdf.

Gulati A, Gayathri, M. 2018: Towards sustainable, productive and profitable agriculture: Case of rice and sugarcane, Working Paper, No. 358, Indian Council for Research on International Economic Relations (ICRIER), New Delhi. [2021-10-15]. http://hdl.handle.net/10419/203692.

Gupta V, Singh V, Jain M K. 2020. Assessment of precipitation extremes in India during the 21st century under SSP1-1.9 mitigation scenarios of CMIP6 GCMs. Journal of Hydrology, 590: 125422, doi: 10.1016/j.jhydrol.2020.125422.

Haj-Amor Z, Acharjee T K, Dhaouadi L, et al. 2020. Impacts of climate change on irrigation water requirement of date palms under future salinity trend in coastal aquifer of Tunisian oasis. Agricultural Water Management, 228: 105843, doi: 10.1016/j.agwat.2019.105843.

Hooper P, Widdowson M, Kelley S. 2010. Tectonic setting and timing of the final Deccan flood basalt eruptions. Geology, 38(9): 839–842.

Irmak S, Odhiambo L O, Specht J E, et al. 2013. Hourly and daily single and basal evapotranspiration crop coefficients as a function of growing degree days, days after emergence, leaf area index, fractional green canopy cover, and plant phenology for soybean. Transactions of the American Society of Agricultural and Biological Engineers, 56(5): 1785–1803.

Jain S K, Singh P K. 2020. Major challenges that climate change will bring to hydrologists. Journal of Hydrologic Engineering, 25(9): 02520002, doi: 10.1061/(ASCE)HE.1943-5584.0001989.

Kim Y H, Min S K, Zhang X, et al. 2020. Evaluation of the CMIP6 multi-model ensemble for climate extreme indices. Weather Climate Extremes, 29: 100269, doi: 10.1016/j.wace.2020.100269.

Konzmann M, Gerten D, Heinke J. 2013. Climate impacts on global irrigation requirements under 19 GCMs, simulated with a vegetation and hydrology model. Hydrological Sciences, 58(1): 88–105.

Li J, Fei L, Li S, et al. 2020. Development of "water-suitable" agriculture based on a statistical analysis of factors affecting irrigation water demand. Science of the Total Environment, 744: 140986, doi: 10.1016/j.scitotenv.2020.140986.

Luo W, Chen M, Kang Y, et al. 2022. Analysis of crop water requirements and irrigation demands for rice: Implications for increasing effective rainfall. Agricultural Water Management, 260: 107285, doi: 10.1016/j.agwat.2021.107285.

Masia S, Trabucco A, Spano D, et al. 2021. A modelling platform for climate change impact on local and regional crop water requirements. Agricultural Water Management, 255: 107005, doi: 10.1016/j.agwat.2021.107005.

Mishra V, Bhatia U, Tiwari A D. 2020. Bias-corrected climate projections for South Asia from Coupled Model Intercomparison Project-6. Scientific Data, 7(1): 1–13.

Mondal S K, Tao H, Huang J, et al. 2021. Projected changes in temperature, precipitation and potential evapotranspiration across Indus River Basin at 1.5–3.0°C warming levels using CMIP6-GCMs. Science of the Total Environment, 789: 147867,

doi: 10.1016/j.scitotenv.2021.147867.

Moseki O, Murray-Hudson M, Kashe K. 2019. Crop water and irrigation requirements of *Jatropha curcas* L. in semi-arid conditions of Botswana: applying the CROPWAT model. Agricultural Water Management, 225: 105754, doi: 10.1016/j.agwat.2019.105754.

Muñoz G, Grieser J. 2006. CLIMWAT 2.0 for CROPWAT. Water Resources, Development and Management Service, 1–5. [2021-10-15]. http://www.juergen-grieser.de/downloads/CLIMWAT_2.pdf.

Peterson T C, Easterling D R. 1994. Creation of homogeneous composite climatological reference series. International Journal of Climatology, 14(6): 671–679.

Peterson T C, Easterling D R, Karl T R, et al. 1998. Homogeneity adjustments of in situ atmospheric climate data: a review. International Journal of Climatology, 18(13): 1493–1517.

Poonia V, Das J, Goyal M K. 2021. Impact of climate change on crop water and irrigation requirements over eastern Himalayan region. Stochastic Environmental Research and Risk Assessment, 35(6): 1175–1188.

Ravindranath N H, Rao S, Sharma N, et al. 2011. Climate change vulnerability profiles for North East India. Current Science, 101(3): 384–394.

Rehana S, Mujumdar P P. 2013. Regional impacts of climate change on irrigation water demands. Hydrological Processes, 27(20): 2918–2933.

Riahi K, Van Vuuren D P, Kriegler E, et al. 2017. The Shared Socioeconomic Pathways and their energy, land use, and greenhouse gas emissions implications: An overview. Global Environmental Change, 42: 153–168.

Rosner B. 1983. Percentage points for a generalized ESD may-outlier procedure. Technometrics, 25: 165–172.

Savva A P, Frenken K. 2002. Crop water requirements and irrigation scheduling. Harare: FAO Sub-Regional Office for East and Southern Africa. [2021-10-15]. https://www.fao.org/3/ai593e/ai593e.pdf.

Schwaller C, Keller Y, Helmreich B, et al. 2021. Estimating the agricultural irrigation demand for planning of non-potable water reuse projects. Agricultural Water Management, 244: 106529, doi: 10.1016/j.agwat.2020.106529.

Shrestha S, Gyawali B, Bhattarai U. 2013. Impacts of climate change on irrigation water requirements for rice–wheat cultivation in Bagmati River Basin, Nepal. Journal of Water and Climate Change, 4(4): 422–439.

Singh D, Gupta R D, Jain S K. 2015a. Study of daily extreme temperature indices over Sutlej Basin, NW Himalayan region, India. Global Nest Journal, 17(2): 301–311.

Singh D, Jain S K, Gupta R D. 2015b. Trend in observed and projected maximum and minimum temperature over NW Himalayan basin. Journal of Mountain Science, 12(2): 417–433.

Singh D, Rai S P, Kumar B, et al. 2016. Study of hydro-chemical characteristics of Lake Nainital in response of human interventions, and impact of twentieth century climate change. Environmental Earth Sciences, 75(20): 1380, doi: 10.1007/s12665-016-6177-1.

Singh R N, Sah S, Das B, et al. 2021. Spatio-temporal trends and variability of rainfall in Maharashtra, India: Analysis of 118 years. Theoretical and Applied Climatology, 143(3): 883–900.

Smith M, Kivumbi D, Heng L K. 2002. Use of the FAO CROPWAT model in deficit irrigation studies. [2022-01-17]. https://www.fao.org/3/Y3655E/Y3655E00.htm.

Sun G. 2013. Impacts of climate change and variability on water resources in the Southeast USA. In: Ingram K T, Dow K, Carter L, et al. Climate of the Southeast United States. NCA Regional Input Reports. Washington DC: Island Press, 210–236.

Todmal R S. 2021. Future climate change scenario over Maharashtra, Western India: Implications of the Regional Climate Model (REMO-2009) for the understanding of agricultural vulnerability. Pure and Applied Geophysics, 178(1): 155–168.

Tubiello F N, Fischer G. 2007. Reducing climate change impacts on agriculture: Global and regional effects of mitigation, 2000–2080. Technological Forecasting and Social Change, 74(7): 1030–1056.

Wada Y, Wisser D, Eisner S, et al. 2013. Multimodel projections and uncertainties of irrigation water demand under climate change. Geophysical Research Letters, 40(17): 4626–4632.

Wellman P, McElhinny M W. 1970. K–Ar age of the Deccan Trap, India. Nature, 227: 595–596.

Widdowson M, Mitchel C. 1999. Large scale stratigraphical, structural and geomorphological constraints for earthquakes in the southern Deccan Traps, India: the case for denudationally-driven seismicity. Geological Society of India, 43: 425–452.

Ye Q, Yang X, Dai S, et al. 2015. Effects of climate change on suitable rice cropping areas, cropping systems and crop water requirements in southern China. Agricultural Water Management, 159: 35–44.

Yu Y, Pi Y, Yu X, et al. 2019. Climate change, water resources and sustainable development in the arid and semi-arid lands of Central Asia in the past 30 years. Journal of Arid Land, 11(1): 1–14.